Molecular Recognition of Histidine-Tagged Molecules by Metal-Chelating Lipids Monitored by Fluorescence Energy Transfer and Correlation Spectroscopy§

Ingmar T. Dorn,† Klaus R. Neumaier,† and Robert Tampé*,†,‡

Contribution from Lehrstuhl für Biophysik, Technische Universität München, James-Franck-Strasse, D-85747 Garching, Germany, and Max-Planck-Institut für Biochemie, Am Klopferspitz 18a, D-82152 Martinsried, Germany

Received October 13, 1997

Abstract: Complex binding of proteins by metal-chelating lipids via surface-exposed or protein-engineered histidines provides an universal and powerful concept for the orientation and two-dimensional crystallization of proteins at self-organized interfaces. To demonstrate pair formation between individual histidine-tagged molecules and chelator lipids on the molecular level, we have synthesized novel lipids bearing both a Ni−NTA chelator and a fluorescent group. These lipids serve as spectroscopic probes to visualize directly the molecular recognition of fluorescence-labeled histidine-tagged peptides by metal-chelating lipids using fluorescence resonance energy transfer (FRET). The molecular docking to chelator lipids assembled in mono- or bilayers is highly specific, revealing only 3% unspecific adsorption and a binding constant of 3 μM. The affinity constant was confirmed by fluorescence correlation spectroscopy (FCS) on single molecules, where the ratio of lipid-bound to free was analyzed by their intrinsically different diffusion times passing through a confocal volume of about 1 fL. By using a model peptide most of the electrostatic and steric contribution to the binding process can be neglected. Therefore, the affinity constant can serve as a standard value for the binding of histidine-tagged proteins to chelator lipid interfaces.

Introduction

Biofunctionalization of interfaces plays an important role in bioanalytical, biochemical, biophysical, and structural studies. Such two-dimensional systems can be studied with well-developed surface-sensitive methods. Therefore, solid surfaces have to be coated by thin films that are functional and biocompatible to avoid distortion of the studied systems caused by unspecific interactions. This surface coating can be achieved by several materials: (i) by adsorbed polymers,[1−4] (ii) by self-assembled monolayers of alkyl silanes[5] or thiols[6,7] on glass or gold, respectively, or (iii) by self-assembled lipid layers. Unlike other thin films, lipid mono- or bilayers can be deposited on nearly every surface by various techniques[8,9] providing biocompatibility, lateral mobility, and two-dimensional patterning. Functional units of biomembranes such as channels, transporters, or other membrane proteins can be reconstituted into vesicles and immobilized at the surface by vesicle fusion.[10−12] Due to their dynamic properties, lipids can be organized in two dimensions by phase segregation,[13] electrical fields,[14] and microfabricated barriers,[15] allowing the generation of structured biofunctional interfaces. Furthermore, lateral diffusion is still possible in supported membranes which is important to mimic processes at or within biological membranes.

* Corresponding author: Robert Tampé, Max-Planck-Institut für Biochemie, Am Klopferspitz 18a, D-82152 Martinsried, Germany. Telephone: +49-89-8578-2646. Fax: +49-89-8578-2641. E-mail: tampe@biochem.mpg.de.

† Technische Universität München.

‡ Max-Planck-Institut für Biochemie.

§ Abbreviations: AcOH, acetic acid; amu, atom mass unit; au, arbitrary units; Boc, *tert*-butyloxycarbonyl; cpm, counts per molecule; DMF, *N*,*N*-dimethylformamide; DCC, *N*,*N*′-dicyclohexylcarbodiimide; DMSO, dimethyl sulfoxide; DODA, dioctadecylamine; EDTA, ethylenediaminetetraacetic acid; EI, electron impact; FAB, fast-atom bombardment; FCS, fluorescence correlation spectroscopy; FRET, fluorescence resonance energy transfer; HEPES, *N*-2-hydroxyethylpiperazine-*N*′-ethanesulfonic acid; IDA, iminodiacetic acid; MeOH, methanol; MS, mass spectrometry; *m*/*z*, mass per charge; NBD, 7-nitro-2,1,3-benzoxadiazol-4-yl; NHS, *N*-hydroxysuccinimide; Ni−NTA, nickel complexed by NTA; NTA, nitrilotriacetic acid; SOPC, 1-stearoyl-2-oleoyl-*sn*-glycero-3-phosphatidylcholine; SPR, surface plasmon resonance; TFA, trifluoroacetic acid; THF, tetrahydrofuran; TLC, thin-layer chromatography; Z, benzyloxycarbonyl.

(1) Löfås, S.; Johnsson, B. *J. Chem. Soc., Chem. Commun.* **1990**, *21*, 1526−1528.

(2) Kühner, M.; Tampé, R.; Sackmann, E. *Biophys. J.* **1994**, *67*, 217−226.

(3) Beyer, D.; Knoll, W.; Ringsdorf, H.; Elender, G.; Sackmann, E. *Thin Solid Films* **1996**, *285*, 825−828.

(4) Elender, G.; Kühner, M.; Sackmann, E. *Biosens. Bioelect.* **1996**, *11*, 565−577.

(5) Brzoska, J. B.; Azousz, I. B.; Rondelez, F. *Langmuir* **1994**, *10*, 4367−4373.

(6) Dubois, L. H.; Nuzzo, R. G. *Annu. Rev. Phys. Chem.* **1992**, *43*, 437−463.

(7) Whitesides, G. M.; Gorman, C. G. *Handbook of Surface Imaging and Visualization*; CRC Press: Boca Raton, FL, 1995; pp 713−733.

(8) Sackmann, E. *Science* **1996**, *271*, 43−48.

(9) Tampé, R.; Dietrich, C.; Elender, G.; Gritsch, S.; Schmitt, L. *Nanofabrication and Biosystems: Integrating Materials Science, Engeneering, and Biology*; Cambridge University Press: London, 1996; pp 201−221.

(10) Brian, A. A.; McConnell, H. M. *Proc. Natl. Acad. Sci. U.S.A.* **1984**, *81*, 6159−6163.

(11) Chan, P.; Lawrence, M. B.; Dustin, M. L.; Ferguson, L. M.; Golan, D. E.; Springer, T. A. *J. Cell Biol.* **1991**, *10*, 245−255.

(12) Salafsky, J.; Groves, J. T.; Boxer, S. G. *Biochemistry* **1996**, *35*, 14773−14781.

(13) McConnell, H. M. *Annu. Rev. Phys. Chem.* **1991**, *42*, 171−95.

(14) Dietrich, C.; Tampé, R. *Biochim. Biophys. Acta* **1995**, *1238*, 183−191.

(15) Groves, J. T.; Ulman, N.; Boxer, S. G. *Science* **1997**, *275*, 651−653.

S0002-7863(97)03562-2 CCC: $15.00
Published on Web 03/13/1998

Functional and structural studies often require the oriented and functional immobilization of proteins which can be achieved in several ways. Physisorption of a protein to a surface via van der Waals, electrostatic, or entropic interactions are highly sensitive toward ionic strength, pH, or temperature. This can lead to multilayer adsorption or a loss of orientation and activity of the protein. Covalent binding of the protein via surface-accessible amino acid residues to a reactive surface often lacks regiospecificity and therefore orientation of the immobilized protein. Additionally, the reactive site of a protein can also be blocked by the immobilization procedure which leads to a reduced activity of the protein.[16] Protein binding via its natural ligand[17,18] is only possible if the ligands can be fixed at the surface and if the process of ligand binding is not the process desired to study. The very affine binding of biotin to streptavidin can also be used for protein immobilization.[17] However, this method requires a rather unspecific chemical biotinylation of the protein. Protein-engineered affinity tags mimicking the biotin moiety overcome this problem. However, they have a drastically reduced affinity to streptavidin[19,20] and an immobilized streptavidin layer as a docking interface is still needed. Immobilized metal ion affinity chromatography (IMAC)[21,22] is a versatile and powerful method for protein purification and characterization. Here, fusion proteins are expressed with a short affinity sequence of five or six histidines (histidine-tag) that binds to metal ion complexes such as nitrilotriacetic acid (NTA) or iminodiacetic acid (IDA). In most cases, the functionality of the protein is preserved. Additionally, the binding is reversible and dissociation can be induced at low pH or by addition of a competitor either for the protein (histidine, imidazole) or the metal ion (EDTA).

We as well as Arnold and colleagues combined the IMAC technique with the unique and fascinating properties of self-organizing systems by introducing the concept of chelator lipids.[23,24] The metal ion and ligand binding properties of the chelator lipid interfaces as well as their dependency on ionic strength, pH, and temperature was examined in detail.[25,26] Specific docking of peptides[27,28] and proteins to chelator lipids via histidine tag[29−31] or surface histidines[24] could be demonstrated. A designed model peptide[32] as well as a DNA binding protein[29] could be organized in two dimensions by phase-segregated chelator lipids. The histidine-tagged protein was found to be fully functional with respect to its specific DNA recognition. Two-dimensional crystallization of proteins at chelator lipid monolayers was reported.[33−36] Metal-chelating surfaces can be produced either by coating with chelator lipids[30] or by modification of different surfaces with NTA.[16,37,38] Although specific binding to self-assembled metal-chelating interfaces has been demonstrated, it was not possible to distinguish between adsorption to the interface and direct pair formation between the chelator and the biomolecule.

In this report, we describe the synthesis of fluorescent chelator lipids which serve as spectroscopic probes to follow the binding process. Due to a distance dependency of fluorescence resonance energy transfer (FRET) in the nanometer range, pair formation between an acceptor-labeled histidine-tagged molecule and a donor-labeled chelator lipid was proven. Molecular recognition was followed at lipid monolayers at the air−water interface as well as at lipid bilayers in vesicle solution. Additionally, specific binding of single histidine-tagged molecules to chelator lipid containing vesicles could be demonstrated by fluorescence correlation spectroscopy (FCS). Due to their intrinsically different diffusion times for passing through a confocal volume, the ratio of free and lipid-bound molecules could be analyzed by the autocorrelation function of the time-dependent fluorescence signal. The quantitative and molecular analysis of this highly specific and oriented docking process provides deeper insights into this versatile and powerful method for reversible immobilization and orientation of proteins at lipid interfaces.

Materials and Methods

Materials. The chemicals used were 1-stearoyl-2-oleoyl-*sn*-glycero-3-phosphatidylcholine (Avanti Polar Lipids, Birmingham, AL), N^{ϵ}-benzyloxycarbonyl-L-lysine *tert*-butyl ester hydrochloride (Bachem, Heidelberg, Germany), Pd/C (5%), fluorescamine, rhodamine 6G, succinic anhydride (Aldrich, Steinheim, Germany), and 5-(and-6)-carboxytetramethylrhodamine succinimidyl ester (Molecular Probes, Eugene, OR). Thin-layer chromatography (TLC) plates (silica gel 60 F_{254}), silica gel (40−63 μM, 230−400 mesh), bromocresol green, and ninhydrin were purchased from Merck (Darmstadt, Germany). All other chemicals and solvents were ordered from Fluka (Neu-Ulm, Germany) and were reagent p.a. grade. Solvent ratios are given in volume/volume if not otherwise stated. The histidine peptide H-GSGSGSGSGSHH-HHHH-OH was synthesized by a solid-phase technique using fluorenylmethoxycarbonyl chemistry. The N-terminus was labeled with tetramethylrhodamine succinimidyl ester in DMSO. The fluorescence-labeled peptide was isolated by reversed-phase HPLC (C_{18}-column) with an gradient from 20 to 80% acetonitrile (0.1% TFA) in water (0.1% TFA). The identity of the labeled peptide was verified by mass spectrometry (electrospray ionization, $M + H^+ = 1977$ m/z).

Analytical Methods. Reactions were monitored by TLC and functional groups were visualized by UV absorbance (Z group), fluorescamine (primary amines), ninhydrin (amines), cobalt isothiocy-

(16) Gershon, P. D.; Khilko, S. *J. Immunol. Methods.* **1995**, *183*, 65−76.
(17) Ahlers, M.; Müller, W.; Reichert, A.; Ringsdorf, H.; Venzmer, J. *Angew. Chem.* **1990**, *102*, 1310−1327.
(18) Madoz, J.; Kuznetzov, B. A.; Medrano, F. J.; Garcia, J. L.; Fernandez, V. M. *J. Am. Chem. Soc.* **1997**, *119*, 1043−1051.
(19) Schmidt, T. G. M.; Koepke, J.; Frank, R.; Skerra, A. *J. Mol. Biol.* **1996**, *255*, 753−766.
(20) Hengsakul, M.; Cass, A. E. G. *J. Mol. Biol.* **1997**, *266*, 621−632.
(21) Porath, J.; Carlsson, J.; Olsson, I.; Belfrage, G. *Nature* **1975**, *258*, 598−599.
(22) Hochuli, E.; Bannwarth, W.; Döbeli, H.; Gentz, R.; Stüber, D. *Bio/Technology* **1988**, *6*, 1321−1325.
(23) Schmitt, L.; Dietrich, C.; Tampé, R. *J. Am. Chem. Soc.* **1994**, *116*, 8485−8491.
(24) Shnek, D. R.; Pack, D. W.; Sasaki, D. Y.; Arnold, F. H. *Langmuir* **1994**, *10*, 2382−2388.
(25) Dietrich, C. Ph.D. Thesis, TU-München 1995.
(26) Pack, D. W.; Arnold, F. H. *Chem. Phys. Lipid.* **1997**, *86*, 135−152.
(27) Gritsch, S.; Neumaier, K.; Schmitt, L.; Tampé, R. *Biosens. Bioelect.* **1995**, *10*, 805−812.
(28) Maloney, K. M.; Shnek, D. R.; Sasaki, D. Y.; Arnold, F. H. *Chem. Biol.* **1996**, *3*, 185−192.
(29) Dietrich, C.; Boscheinen, O.; Scharf, K. D.; Schmitt, L.; Tampé, R. *Biochemistry* **1996**, *35*, 1100−1105.
(30) Schmitt, L.; Bohanon, T. M.; Denzinger, S.; Ringsdorf, H.; Tampé, R. *Angew. Chem., Int. Ed. Engl.* **1996**, *35*, 317−320.
(31) Ng, K.; Pack, D. W.; Sasaki, D. Y.; Arnold, F. H. *Langmuir* **1995**, *11*, 4048−4055.
(32) Dietrich, C.; Schmitt, L.; Tampé, R. *Proc. Natl. Acad. Sci. U.S.A.* **1995**, *92*, 9014−9018.
(33) Kubalek, E. W.; Le Grice, F. J.; Brown, P. O. *J. Struct. Biol.* **1994**, *113*, 117−123.
(34) Frey, W.; Schief, W. R.; Pack, D. W.; Chen, C. T.; Chilkoti, A.; Stayton, P.; Vogel, V.; Arnold, F. H. *Proc. Natl. Acad. Sci. U.S.A.* **1996**, *93*, 4937−4941.
(35) Pack, D. W.; Chen, G.; Maloney, K. M.; Chen, C.; Arnold, F. H. *J. Am. Chem. Soc.* **1997**, *119*, 2479−2487.
(36) Barklis, E.; McDermott, J.; Wilkens, S.; Schabtach, E.; Schmid, M. F.; Fuller, S.; Karanjia, S.; Love, Z.; Jones, R.; Rui, Y.; Zhao, X.; Thompson, D. *EMBO J.* **1997**, *16*, 1199−1213.
(37) O'Shannessy, D. J.; O'Donnell, K. C.; Martin, J.; Brigham-Burke, M. *Anal. Biochem.* **1995**, *229*, 119−124.
(38) Sigal, G. B.; Bamdad, C.; Barberis, A.; Strominger, J.; Whitesides, G. M. *Anal. Chem.* **1996**, *68*, 490−497.

anate (amines, amides), and bromocresol green (acids and bases). ^{1}H NMR (500 MHz) and ^{13}C NMR (100 MHz) spectra were recorded on Bruker AM 500 and AM 400, respectively. Chemical shifts (δ) are given in parts per million relative to the $CDCl_3$ signal. Mass spectrometry was performed at a Finnigan MAT (Forster City, CA) either in the electron impact (EI), in the electrospray, or in the fast-atom bombardment (FAB) ionization mode.

Film Balance Measurements. Epifluorescence film balance measurements were performed on a self-built instrument as previously described.[32] The trough (Teflon) was 220 mm × 30 mm and carried a subphase volume of 25 mL. The surface tension was measured by a Wilhelmy system, and the temperature was controlled by peltier elements. The speed of the movable barrier and the lateral pressure were computer-controlled. The film balance was equipped with an epifluorescence microscope. Fluorescence was excited by a HBO 50 lamp (Zeiss, Kochel, Germany). The fluorescence filter set (Zeiss) consisted of an excitation filter (450−490 nm), a dichroitic mirror (510 nm), and an emission filter (long pass >520 nm). The fluorescence microscope was interfaced to a monochromator via a glass fiber technique. Intensities were measured by a photomultiplier working in the single photon counting mode. For all experiments, degassed and sterile filtered HEPES buffers (10 mM HEPES, 150 mM NaCl, pH 7.5) were used if not stated otherwise. The NTA lipids were preloaded with nickel ions in organic solution by adding equimolar amounts of a methanol solution of $NiCl_2 \cdot 6H_2O$. In experiments in which the buffer contained EDTA, the unloaded NTA lipid was used. For the binding experiments, the lipid monolayer was compressed to a surface pressure of 20 mN/m at a temperature of 22 °C. The histidine peptide was injected into the subphase while the area was kept constant. The spectra were measured in the sample/reference (s/r) mode and baseline corrected. The baseline was recorded prior to each experiment. To reach equilibrium the spectra were recorded 2 or 4 h after addition of the histidine peptide or EDTA, respectively.

Vesicle Preparation. Appropriate molar ratios of lipid were mixed in chloroform/methanol (6:1), and the organic solvent was removed in a vacuum. The dry lipid was swollen in HEPES buffer to a final concentration of 6.7 mM at room temperature for 2 h and then extruded 21 times through 100-nm filters (LiposoFast-Basic, Avestin, Ottawa, Canada). The lipid concentration was measured by UV absorption at 490 nm according to the absorption maximum of NBD.

Fluorescence Spectroscopy in Vesicle Solution. Fluorescence spectra were recorded at a donor concentration of 3.25 μM and at acceptor concentrations of 0.5, 1, 2.5, 5, and 10 μM on a Fluorolog-2 (Spex Industries Inc., Edison, NJ) with an excitation at 450 nm to minimize direct excitation of the acceptor. We scanned the emission from 490 to 620 nm in 2-nm steps with an integration time of 1 s per step. All spectra were recorded at room temperature in the s/r mode.

Fluorescence Correlation Spectroscopy. FCS measurements were performed on a Zeiss ConfoCor (Carl Zeiss Jena, Jena, Germany) equipped with a Nd:YAG laser (10 mW, excitation at 532 nm). The instrument was controlled by FCS Access software, and the autocorrelation functions were analyzed with FCS Access Fit software.[39] The diameter of the pinhole was adjusted to 50 μM and the geometry of the confocal element was determined by a one-component fit (eq 1) to the correlation curve of rhodamine 6G. To determine an affinity constant, we titrated 15 nM rhodamine-labeled histidine peptide with an increasing concentration of SOPC vesicles doped with 3 mol % Ni−NTA lipid. Each point on the titration curve corresponds to the average of six measurements. The time-dependent fluorescence signal was collected over a period of 60 s. The autocorrelation curves were fitted by a two-component model (eq 2) as described.[39]

$$G(t) = 1 + \frac{1 - \mathrm{TA}(1 - e^{-t/t_0})}{N[1 - \mathrm{TA}]} \frac{1}{1 + (t/\tau)} \frac{1}{[1 + S^2(t/\tau)]^{1/2}} \quad (1)$$

$$G(t) = 1 + \frac{1 - \mathrm{TA}(1 - e^{-t/t_0})}{N[1 - \mathrm{TA}]} \times \left[\frac{1 - y}{1 + (t/\tau_1)} \frac{1}{[1 + S^2(t/\tau_1)]^{1/2}} + \frac{y}{1 + (t/\tau_2)} \frac{1}{[1 + S^2(t/\tau_2)]^{1/2}}\right] \quad (2)$$

In eqs 1 and 2, N is the number of molecules in the confocal volume, τ the diffusion time through the confocal volume (in eq 2, of component 1 or 2, respectively), S the structural parameter, TA the fraction of molecules in the triplet state, t_0 the time constant of the triplet state, and y the fraction of molecules with a diffusion time τ_2.

Diffusion coefficients D were calculated by eq 3,

$$D = \omega_1^2/4\tau \quad (3)$$

where ω_1 corresponds to the radius of the elliptical confocal volume perpendicular to the optical axis and τ to the diffusion time through the confocal volume.

Experimental Section

Synthesis of the NBD-Labeled Chelator Lipid. Synthesis of *N*-(*tert*-Butyloxycarbonyl)-12-aminododecanoic Acid (2). 12-Aminododecanoic acid (**1**) (430 mg, 2 mmol) was suspended in 20 mL of absolute methanol and 400 μL of triethylamine. A solution of 872 mg (4 mmol) of di-*tert*-butyl dicarbonate in 10 mL of absolute methanol was added. After being stirred for 1 h at 60 °C, the reaction mixture cleared up and the CO_2 production stopped. The solvent was removed in a vacuum, and the remaining oil was dissolved in 20 mL of chloroform and extracted twice with hydrochloric acid (pH 2.5). The organic phase was dried over anhydrous sodium sulfate, and the solvent as well as the *tert*-butyl alcohol was removed in a vacuum. Yield: 605 mg (1.92 mmol) of **2**; 96%. TLC: $R_f = 0.61$ in $CHCl_3$/MeOH (15:1). ^{1}H NMR (400 MHz, $CDCl_3$): $\delta = 1.20$ (m, 16 H, Boc-NHCH$_2$-CH$_2$(C**H**$_2$)$_8$CH$_2$COOH), $\delta = 1.36$ (s, 9 H, (**H**$_3$C)$_3$COCONH−), $\delta = 1.55$ (q, 2 H, Boc-NHCH$_2$C**H**$_2$(CH$_2$)$_8$CH$_2$COOH), $\delta = 2.26$ (t, 2 H, Boc-NHCH$_2$CH$_2$(CH$_2$)$_8$C**H**$_2$COOH), $\delta = 3.02$ (bm, 2 H, Boc-NHC**H**$_2$-CH$_2$(CH$_2$)$_8$)CH$_2$COOH), $\delta = 4.49$ (bs, 1 H, Boc-N**H**CH$_2$CH$_2$(CH$_2$)$_8$-CH$_2$COOH). ^{13}C NMR (100 MHz, $CDCl_3$): $\delta = 25.37, 27.45, 29.12, 29.71-30.10, 30.69$ ((H$_3$**C**)$_3$COCONHCH$_2$**C**H$_2$(**C**H$_2$)$_8$CH$_2$COOH), $\delta = 34.72$ (**C**H$_2$COOH), $\delta = 41.34$ (CONH**C**H$_2$), $\delta = 79.77$ ((H$_3$C)$_3$-**C**OCO), $\delta = 156.76$ ((H$_3$C)$_3$CO**C**ONH), $\delta = 179.94$ (CH$_2$**C**OOH). MS (EI, $C_{17}H_{33}NO_4$): $M^+ = 315$ *m*/*z*.

Synthesis of *N*-(*N*′-(*tert*-Butyloxycarbonyl)-12-aminododecanoyl)-octadecylamide (3). After dissolving 605 mg (1.92 mmol) of compound **2** and 845 mg (3.84 mmol) of 2,2′-dipyridyl disulfide in 25 mL of absolute chloroform, 516 mg (1.92 mmol) of octadecylamine, 1006 mg (3.84 mmol) of triphenylphosphine, and 300 μL of triethylamine were added in 25 mL of absolute chloroform. After the mixture was stirred for 4 h at room temperature, the solvent was evaporated and the product was recrystallized from acetone. Yield: 1000 mg of **3**, 92%. TLC: $R_f = 0.84$ in $CHCl_3$/MeOH (50:1). ^{1}H NMR (400 MHz, $CDCl_3$): $\delta = 0.87$ (t, 3H, **H**$_3$C−), $\delta = 1.25$ (m, 46 H, H$_3$C(C**H**$_2$)$_{15}$-CH$_2$−, Boc-NH(CH$_2$)$_2$(C**H**$_2$)$_8$CH$_2$−), $\delta = 1.43$ (m, 11 H, (**H**$_3$C)$_3$-CCONHCH$_2$C**H**$_2$−), $\delta = 1.60$ (q, 2 H, H$_3$C(CH$_2$)$_{15}$C**H**$_2$CH$_2$NHCO−), $\delta = 2.14$ (dd, 2 H, H$_3$C(CH$_2$)$_{17}$NHCOC**H**$_2$−), $\delta = 3.09$ (dd, 2H, Boc-NHC**H**$_2$−), $\delta = 3.22$ (dd, 2 H, H$_3$C(CH$_2$)$_{16}$C**H**$_2$NHCO−), $\delta = 4.51$ (bs, 1 H, Boc-N**H**−), $\delta = 5.48$ (bs, 1 H, H$_3$C(CH$_2$)$_{17}$N**H**CO−). ^{13}C NMR (100 MHz, $CDCl_3$): $\delta = 14.77$ (H$_3$**C**−), $\delta = 23.35, 26.49, 27.44, 27.60, 29.10, 29.97-30.25, 30.35, 30.73, 32.59$ (H$_3$C(**C**H$_2$)$_{16}$CH$_2$-NHCO**C**H$_2$(**C**H$_2$)$_9$CH$_2$NHCOOC(**C**H$_3$)$_3$), $\delta = 40.15$ (H$_3$C(CH$_2$)$_{16}$**C**H$_2$-NHCO−), $\delta = 41.30$ (Boc-NH**C**H$_2$−), $\delta = 79.64$ ((H$_3$C)$_3$**C**OCO−), $\delta = 156.66$ ((H$_3$C)$_3$CO**C**O−), $\delta = 173.68$ (H$_3$C(CH$_2$)$_{17}$NH**C**O−). MS (EI, $C_{35}H_{70}N_2O_3$): $M^+ = 566$ *m*/*z*.

Synthesis of *N*-(*N*′-Methyl-12-aminododecyl)octadecylamine (4). A $LiAlH_4$−THF solution (44.2 mL, 0.2 M) was added drop by drop at 0 °C to a solution of 1000 mg (1.77 mmol) of compound **3** in 200 mL of THF (freshly distilled over CaH_2) under an inert gas atmosphere. The reaction mixture was refluxed for 3 h and then cooled to 0 °C. The excess of $LiAlH_4$ was quenched by adding 336 μL of water and 336 μL of NaOH (15% in water, w/w) and 1 mL of water. The precipitated $Al(OH)_3$ is filtered off and washed three times with hot chloroform. The combined organic phases were dried over anhydrous sodium sulfate, and the solvent was removed in a vacuum. The product was recrystallized from THF. Yield: 734 mg (1.58 mmol) of **4**, 89%.

(39) EVOTEC *FCS Access Fit Software*; EVOTEC: Hamburg, Germany, 1996.

TLC: $R_f = 0.54$ in $CHCl_3$/MeOH/AcOH (40:8:1). ^{1}H NMR (400 MHz, $CDCl_3$): $\delta = 0.87$ (t, 2 H, $\mathbf{H}_3C(CH_2)_{17}NH-$), $\delta = 1.18$ (s, 1 H, $H_3C(CH_2)_{17}N\mathbf{H}-$), $\delta = 1.27$ (m, 46 H, $H_3C(C\mathbf{H}_2)_{15}CH_2CH_2NHCH_2CH_2(C\mathbf{H}_2)_8-$), $\delta = 1.47$ (m, 6 H, $H_3C(CH_2)_{15}C\mathbf{H}_2CH_2NHCH_2C\mathbf{H}_2(CH_2)_8C\mathbf{H}_2-$), $\delta = 2.43$ (s, 3 H, $\mathbf{H}_3CNH(CH_2)_{12}NH-$), $\delta = 2.55$ (t, 4 H, $-C\mathbf{H}_2NHC\mathbf{H}_2-$), $\delta = 2.58$ (t, 2 H, $H_3CNHC\mathbf{H}_2-$). ^{13}C NMR (100 MHz, $CDCl_3$): $\delta = 14.10$ ($H_3\mathbf{C}-$), $\delta = 22.69, 27.36, 27.45, 29.36, 29.60-29.68, 29.97, 30.24, 31.92$ ($H_3C(\mathbf{C}H_2)_{16}CH_2NHCH_2(\mathbf{C}H_2)_{10}CH_2NHCH_3$), $\delta = 36.58$ ($H_3\mathbf{C}NH(CH_2)_{12}NH-$), $\delta = 50.19$ ($-\mathbf{C}H_2NH\mathbf{C}H_2-$), $\delta = 52.26$ ($H_3CNH\mathbf{C}H_2-$). MS (FAB, $C_{31}H_{66}N_2$): M + H^+ = 467 *m/z*.

Synthesis of *N*-(*N*′-Methyl-*N*′-(*tert*-butyloxycarbonyl)-12-aminododecyl)octadecylamine (5). Di-*tert*-butyl dicarbonate (349 mg, 1.6 mmol) in 25 mL of absolute chloroform/methanol (9:1) was added to a solution of 734 mg (1.58 mmol) of compound **4** and 700 μL of triethylamine in 50 mL of absolute chloroform/methanol (9:1) at −20 °C over a period of 2 h. Thereafter the reaction was stopped by adding 50 mL of cold hydrochloric acid (pH 2.5). The cold bath was removed, and the reaction mixture was stirred for an additional 10 min at room temperature. After phase separation, the organic phase was extracted with 1 N NaOH and dried over anhydrous sodium sulfate, and the solvent was removed in a vacuum. The product was purified by silica gel column chromatography using $CHCl_3$/MeOH (15:1) as the eluant. Yield: 715 mg (1.26 mmol) of **5**, 80%. TLC: $R_f = 0.48$ in $CHCl_3$/MeOH (15:1). ^{1}H NMR (400 MHz, $CDCl_3$): $\delta = 0.88$ (t, 3 H, $\mathbf{H}_3C(CH_2)_{17}NH-$), $\delta = 1.11$ (s, 1 H, $-CH_2N\mathbf{H}CH_2-$), $\delta = 1.25$ (m, 46 H, $H_3C(C\mathbf{H}_2)_{15}CH_2CH_2NHCH_2CH_2(C\mathbf{H}_2)_8CH_2-$), $\delta = 1.45$ (s, 9H, $(\mathbf{H}_3C)_3COCON(CH_3)-$), $\delta = 1.49$ (q, 2 H, Boc-N(CH_3)$CH_2C\mathbf{H}_2-$), $\delta = 1.65$ (q, 4 H, $-C\mathbf{H}_2CH_2NHCH_2C\mathbf{H}_2-$), $\delta = 2.74$ (bt, 4 H, $CH_2C\mathbf{H}_2NHC\mathbf{H}_2CH_2-$), $\delta = 2.83$ (s, 3 H, Boc-N($C\mathbf{H}_3$)−), $\delta = 3.18$ (bdd, 2 H, Boc-N(CH_3)$C\mathbf{H}_2-$). ^{13}C NMR (100 MHz, $CDCl_3$): $\delta = 14.80$ ($H_3\mathbf{C}-$), $\delta = 23.39, 27.42, 27.96, 28.52, 29.18, 29.34, 30.12-30.38, 32.62$ ($H_3C(\mathbf{C}H_2)_{16}CH_2NHCH_2(\mathbf{C}H_2)_{10}-$), $\delta = 34.73$ (Boc-N(CH_3)$\mathbf{C}H_2-$), $\delta = 49.44, 49.98$ ($-\mathbf{C}H_2NH\mathbf{C}H_2-$), $\delta = 79.71$ (($H_3C\mathbf{C}CON(CH_3)-$), $\delta = 156.70$ (($H_3C)_3CO\mathbf{C}ON(CH_3)-$). MS (FAB, $C_{36}H_{74}N_2O_2$): M + H^+ = 567 *m/z*.

Synthesis of *N*-Succinyl-*N*-(*N*′-methyl-*N*′-(*tert*-butyloxycarbonyl)-12-aminododecyl)octadecylamine (6). A solution of compound **5** (715 mg, 1.26 mmol), 400 μL of triethylamine, and 189 mg (1.89 mmol) of succinic anhydride in 40 mL of absolute chloroform was stirred at room temperature for 3 h. The organic phase was extracted twice with 1 N NaOH and dried over anhydrous sodium sulfate. The solvent was removed in a vacuum. Yield: 772 mg (1.16 mmol), 92%. TLC: $R_f = 0.53$ in $CHCl_3$/AcOH (25:1). ^{1}H NMR (400 MHz, $CDCl_3$): $\delta = 0.88$ (t, 3 H, $\mathbf{H}_3C(CH_2)_{17}N-$), $\delta = 1.25$ (m, 46 H, $H_3C(C\mathbf{H}_2)_{15}CH_2CH_2N(COCH_2CH_2COOH)CH_2CH_2(C\mathbf{H}_2)_8-$), $\delta = 1.45$ (s, 9 H, $(\mathbf{H}_3C)_3COCON-$), $\delta = 1.46-1.60$ (m, 6 H, $-C\mathbf{H}_2CH_2N(COCH_2CH_2COOH)CH_2C\mathbf{H}_2(CH_2)_8C\mathbf{H}_2CH_2N(CH_3)Boc$), $\delta = 2.68$ (m, 4 H, $NCOC\mathbf{H}_2C\mathbf{H}_2COOH$), $\delta = 3.18$ (dd, 2 H, Boc-N(CH_3)$C\mathbf{H}_2-$), $\delta = 3.23, 3.31$ (2 dd, 2*2 H, $-C\mathbf{H}_2N(CO(CH_2)_2COOH)C\mathbf{H}_2-$). ^{13}C NMR (100 MHz, $CDCl_3$): $\delta = 14.80$ ($H_3\mathbf{C}-$),$\delta = 23.38, 27.39, 27.59, 27.70, 28.75, 29.18, 29.51, 30.05, 30.24-30.38, 32.62$ ($H_3C(\mathbf{C}H_2)_{16}CH_2N(CO(CH_2)_2COOH)CH_2(\mathbf{C}H_2)_{10}-$), $\delta = 34.74$ (Boc-N(CH_3)$\mathbf{C}H_2-$), $\delta = 47.36$ ($-\mathbf{C}H_2N(CO-(CH_2)_2COOH)\mathbf{C}H_2-$), $\delta = 49.00$ ($N(COCH_2\mathbf{C}H_2COOH$), $\delta = 49.50$ ($-CH_2N(CO\mathbf{C}H_2CH_2COOH)CH_2-$), $\delta = 79.79$ (($H_3C)_3\mathbf{C}OCON-$), $\delta = 156.60$ (($H_3C)_3CO\mathbf{C}ON$), $\delta = 172.86$ ($-CH_2N(\mathbf{C}O(CH_2)_2COOH)CH_2-$), $\delta = 175.55$ ($-CH_2N(CO(CH_2)_2\mathbf{C}OOH)CH_2-$). MS (FAB, $C_{40}H_{78}N_2O_5$): M + H^+ = 667 *m/z*.

Synthesis of *N*-Succinyl-*N*-(*N*′-methyl-12-aminododecyl)octadecylamine (7). The protected ω-amino acid **6** (772 mg, 1.16 mmol) was dissolved in 44 mL of chloroform/trifluoroacetic acid (9:1) and stirred at room temperature. After completion of the gas production (12 h), the organic phase was extracted with 0.01 N NaOH until the aqueous phase remained basic. The combined organic phases were dried over sodium sulfate, and the solvent was removed in a vacuum. Yield: 617 mg (1.09 mmol) of **7**, 94%. TLC: $R_f = 0.31$ in $CHCl_3$/MeOH (9:1). ^{1}H NMR (400 MHz, $CDCl_3$): $\delta = 0.87$ (t, 3 H, $\mathbf{H}_3C(CH_2)_{17}N-$), $\delta = 1.25$ (m, 46 H, $H_3C(C\mathbf{H}_2)_{15}CH_2CH_2N(CO(CH_2)_2COOH)CH_2CH_2(C\mathbf{H}_2)_8-$), $\delta = 1.48, 1.55$ (2 q, 2*2 H, $CH_2C\mathbf{H}_2N(CO(CH_2)_2COOH)CH_2C\mathbf{H}_2-$), $\delta = 1.68$ (q, 2 H, $H_3C^+NH_2CH_2C\mathbf{H}_2-$), $\delta = 2.59$ (m, 4 H, $-CH_2N(CO(C\mathbf{H}_2)_2COOH)CH_2-$), $\delta = 2.64$ (d, 3 H, $\mathbf{H}_3C^+NH_2CH_2CH_2-$), $\delta = 2.90$ (dt, 2 H, $H_3C^+NH_2C\mathbf{H}_2CH_2-$), $\delta = 3.24$ (2 dd, 4 H, $-C\mathbf{H}_2N(CO(CH_2)_2COOH)C\mathbf{H}_2-$), $\delta = 7.70-8.40$ (b, $H_3C^+N\mathbf{H}_2CH_2-$). ^{13}C NMR (100 MHz, $CDCl_3$): $\delta = 14.77$ ($H_3\mathbf{C}-$), $\delta = 23.34, 26.98, 27.13, 27.41, 27.62, 27.78, 28.20, 28.40, 29.13, 29.26, 29.39, 29.55, 29.64, 30.02, 30.13-30.35, 31.42, 31.50, 32.58$ ($H_3C(\mathbf{C}H_2)_{16}CH_2N(CO(CH_2)_2COOH)CH_2(\mathbf{C}H_2)_{10}-$), $\delta = 33.61$ ($H_3\mathbf{C}^+NH_2CH_2-$), $\delta = 46.95$ ($-\mathbf{C}H_2N(CO(CH_2)_2COOH)\mathbf{C}H_2-$), $\delta = 48.68$ ($-CH_2N(CO(\mathbf{C}H_2)_2COOH)CH_2-$), $\delta = 50.09$ ($H_3C^+NH_2\mathbf{C}H_2-$), $\delta = 172.73$ ($N(\mathbf{C}O(CH_2)_2COOH)$), $\delta = 177.66$ ($N(CO(CH_2)_2\mathbf{C}OOH$). MS (FAB, $C_{35}H_{70}N_2O_3$): M + H^+ = 667 *m/z*.

Synthesis of *N*-Succinyl-*N*-(*N*′-methyl-*N*′-(7-nitro-2,1,3-benzoxadiazol-4-yl)-12-aminododecyl)octadecylamine (8). Compound **7** (617 mg, 1.09 mmol) and 300 μL of triethylamine were dissolved in 40 mL of chloroform, and 239 mg (1.20 mmol) of 7-nitro-2,1,3-benzoxadiazol-4-chloride was added under the exclusion of light. After 12 h of stirring at room temperature, the organic phase was extracted three times with 1 N hydrochloric acid and dried over anhydrous sodium sulfate, and the solvent was removed in a vacuum. The product **8** was recrystallized from acetone. Yield: 715 mg (0.98 mmol) of **8**, 90%. TLC: $R_f = 0.45$ in $CHCl_3$/MeOH (15:1). ^{1}H NMR (400 MHz, $CDCl_3$): $\delta = 0.87$ (t, 3 H, $\mathbf{H}_3C(CH_2)_{17}N$), $\delta = 1.26$ (m, 46 H, $H_3C(C\mathbf{H}_2)_{15}CH_2CH_2N(CO(CH_2)_2COOH)CH_2CH_2(C\mathbf{H}_2)_8-$), $\delta = 1.53$ (m, 4 H, $-C\mathbf{H}_2CH_2N(CO(CH_2)_2COOH)CH_2C\mathbf{H}_2-$), $\delta = 1.75$ (q, 2 H, NBD-N(CH_3)$CH_2C\mathbf{H}_2-$), $\delta = 2.67$ (m, 4 H, $-CH_2N(CO(C\mathbf{H}_2)_2COOH)CH_2-$), $\delta = 3.23, 3.30$ (2 dd, 2*2 H, $-C\mathbf{H}_2N(CO(CH_2)_2COOH)C\mathbf{H}_2$), $\delta = 3.48$ (m, 3 H, NBD-N($C\mathbf{H}_3$)CH_2-), $\delta = 4.05$ (m, 2 H, NBD-N(CH_3)$C\mathbf{H}_2-$), $\delta = 6.07$ (d, 1 H, H-6), $\delta = 8.41$ (d, 1 H, H-5). ^{13}C NMR (100 MHz, $CDCl_3$): $\delta = 14.77$ ($H_3\mathbf{C}-$), $\delta = 23.35, 27.30, 27.56, 27.64, 28.29, 28.70, 29.49, 29.91, 30.01, 30.12-30.35, 31.04, 32.59$ ($H_3C(\mathbf{C}H_2)_{15}CH_2N(CO(CH_2)_2COOH)CH_2(\mathbf{C}H_2)_{10}-$), $\delta = 42.13$ (NBD-N($\mathbf{C}H_3$)CH_2-), $\delta = 47.31$ ($-\mathbf{C}H_2N(CO(CH_2)_2COOH)\mathbf{C}H_2-$), $\delta = 48.97$ ($-CH_2N(CO(\mathbf{C}H_2)_2COOH)CH_2-$), $\delta = 56.66$ (NBD-N(CH_3)$\mathbf{C}H_2-$), $\delta = 101.61$ (C-6), $\delta = 122.76$ (C-5), $\delta = 136.06$ (C-1), $\delta = 145.19$ (C-2), $\delta = 145.55$ (C-3), $\delta = 146.13$ (C-4), $\delta = 172.78$ ($-CH_2N(\mathbf{C}O(CH_2)_2COOH)CH_2$), $\delta = 175.99$ ($-CH_2N(CO-(CH_2)_2\mathbf{C}OOH)CH_2-$). MS (FAB, $C_{41}H_{71}N_5O_6$): M + H^+ = 730 *m/z*.

Synthesis of N^{α},N^{α}-Bis[(*tert*-butyloxycarbonyl)methyl]-N^{ϵ}-benzyloxycarbonyl-L-lysine *tert*-Butyl Ester (10). A solution of 535 mg (1.65 mmol) N^{ϵ}-benzyloxycarbonyl-L-lysine *tert*-butyl ester hydrochloride, 1.33 mL of triethylamine, and 3.2 g (16.5 mmol) of bromoacetic acid *tert*-butyl ester was stirred in 20 mL of DMF for 4 days at 50 °C. The solvent and the excess of bromoacetic acid *tert*-butyl ester was removed in a vacuum, and the remaining oil was extracted six times with hexane. The combined organic phases were collected and the solvent was removed in a vacuum. Yield: 614 mg (1.09 mmol) of **10**, 66%. TLC: $R_f = 0.70$ in $CHCl_3$/MeOH (100:1). ^{1}H NMR (400 MHz, $CDCl_3$): $\delta = 1.42$ (s, 18 H, $((\mathbf{H}_3C)_3COCOCH_2)_2N-$), $\delta = 1.45$ (s, 9H, $(\mathbf{H}_3C)_3COCOCH_2CH-$) $\delta = 1.53$ (m, 4 H, $Z\text{-}NHCH_2(C\mathbf{H}_2)_2-$), $\delta = 1.64$ (m, 2 H, $Z\text{-}NH(CH_2)_3C\mathbf{H}_2-$), $\delta = 3.19$ (q, 2 H, $Z\text{-}NHC\mathbf{H}_2-$), $\delta = 3.31$ (t, 1 H, $Z\text{-}NH(CH_2)_4C\mathbf{H}-$), $\delta = 3.46$ (dd, 4 H, $((H_3C)_3COCOC\mathbf{H}_2)_2N-$), $\delta = 5.08$ (s, 2 H, $C_6H_5C\mathbf{H}_2OCONH-$), $\delta = 7.32$ (m, 5 H, $C_6\mathbf{H}_5CH_2OCONH-$). ^{13}C NMR (100 MHz, $CDCl_3$): $\delta = 23.68, 28.77, 28.88-29.90, 30.74$ ($Z\text{-}NHCH_2(\mathbf{C}H_2)_3-$, $((\mathbf{C}H_3)_3COCO)_3$), $\delta = 41.47$ ($Z\text{-}NH\mathbf{C}H_2-$), $\delta = 54.56$ ($-N(\mathbf{C}H_2)COOC(CH_3)_2$), $\delta = 65.83$ ($-\mathbf{C}HN(CH_2COOC(CH_3)_3)_2$), $\delta = 67.10$ ($C_6H_5\mathbf{C}H_2OCONH-$), $\delta = 81.44$ ($-N(CH_2COO\mathbf{C}(CH_3)_3)_2$), $\delta = 81.85$ (($H_3C)_3\mathbf{C}OCOCH-$), $\delta = 128.60-128.72, 129.10$ (C-2, C-3, C-4, C-5, C-6), $\delta = 137.47$ (C-1), $\delta = 157.14$ ($C_6H_5CH_2O\mathbf{C}ONH-$), $\delta = 171.39$ ($N(CH_2\mathbf{C}OOC(CH_3)_3)_2$), $\delta = 173.10$ (($H_3C)_3CO\mathbf{C}OCH$). MS (FAB, $C_{30}H_{48}N_2O_8$): M + H^+ = 565 *m/z*.

Synthesis of N^{α},N^{α}-Bis[(*tert*-butyloxycarbonyl)methyl]-L-lysine *tert*-Butyl Ester (11). The Z-protected amine **10** (614 mg, 1.09 mmol) was dissolved in 50 mL of $CHCl_3$/AcOH (25:1). After 15 mg of Pd/C (5% Pd) was added, compound **10** was hydrogenated at room temperature and normal pressure for 2 h. The catalyst was filtered off, and the reaction mixture was extracted twice with 1 N NaOH. The combined organic phases were dried over anhydrous sodium sulfate, and the organic solvent was removed in a vacuum. Yield: 421 mg (0.98 mmol) of **11**, 90%. TLC: $R_f = 0.32$ in $CHCl_3$/MeOH (3:1). ^{1}H NMR (400 MHz, $CDCl_3$): $\delta = 1.43$ (s, 18 H, $((\mathbf{H}_3C)_3COCOCH_2)_2N-$), $\delta = 1.44$ (s, 9H, $(\mathbf{H}_3C)_3COCOCH_2CH-$), $\delta = 1.46, 1.63$ (2*m,

2*2 H, $H_2N(CH_2)_2(CH_2)_2-$), δ = 1.73 (bm, 2 H, $H_2NCH_2CH_2-$), δ = 2.68 (t, 2 H, H_2NCH_2-), δ = 3.29 (t, 2 H, $H_2N(CH_2)_4CH-$), δ = 3.45 (dd, 4 H, $-N(CH_2COOC(CH_3)_3)_2$). ^{13}C NMR (100 MHz, $CDCl_3$): δ = 23.88, 28.80−28.89, 31.18, 33.89 ($H_2NCH_2(CH_2)_3-$, $((CH_3)_3COCO-)_3$), δ = 42.61 (H_2NCH_2-), δ = 54.46 ($-N(CH_2-COOC(CH_3)_3)_2$), δ = 65.96 ($H_2N(CH_2)_4CH-$), δ = 81.31 ($-N(CH_2-COOC(CH_3)_3)_2$), δ = 81.66 ($((CH_3)_3COCOCH)_3$), δ = 171.39 ($-N(CH_2COOC(CH_3)_3)_2$), δ = 173.10 ($(CH_3)_3COCOCH$). MS (FAB, $C_{22}H_{42}N_2O_6$): M + H^+ = 431 *m/z*.

Synthesis of N^{α},N^{α}-Bis[(*tert*-butyloxycarbonyl)methyl]-N^{ϵ}-[*N*-[*N*′-methyl-*N*′-(7-nitro-2,1,3-benzoxadiazol-4-yl)-12-aminododecyl]octadecylamine]succinyl-L-lysine *tert*-Butyl Ester (12). Under the exclusion of light, 715 mg (0.98 mmol) of compound **8** was dissolved in 20 mL of absolute CH_2Cl_2 and 202 mg (0.98 mmol) of dicyclohexylcarbodiimide, 113 mg (0.98 mmol) of *N*-hydroxysuccinimide and 15 mg of 4-(dimethylamino)pyridine in 10 mL of absolute acetone were added. After 4 h of stirring at room temperature, the precipitated urea was filtered off and 421 mg (0.98 mmol) of compound **11** and 390 μL of triethylamine in 20 mL of absolute CH_2Cl_2 were added. The reaction was stirred for 5 h. Thereafter the solvent was removed in a vacuum. The product was recrystallized from acetone. Yield: 1005 mg (0.88 mmol) of **12**, 90%. TLC: R_f = 0.29 in $CHCl_3$/MeOH (75:1). ^{1}H NMR (400 MHz, $CDCl_3$): δ = 0.89 (t, 3 H, $H_3C(CH_2)_{17}-$), δ = 1.18−1.40 (m, 46 H, $H_3C(CH_2)_{15}-$, NBD-$N(CH_3)(CH_2)_2CH_2)_8-$), δ = 1.42 (s, 18 H, $((H_3C)_3COCOCH_2)_2N-$), δ = 1.44 (s, 9H, $(H_3C)_3COCOCH_2-CH-$), δ = 1.45−1.67 (m, 10 H, $-(CH_2)CH_2N(CO(CH_2)_2CONHCH_2-(CH_2)_2)(CH_2)CH_2-$, NBD-$N(CH_3)CH_2CH_2-$), δ = 1.74 (q, 2 H, $-CO(CH_2)_2CONH(CH_2)_3(CH_2)CH-$), δ = 2.50, 2.62 (2 t, 2*2 H, $-CO(CH_2)_2CONH-$), δ = 3.15−3.29 (m, 7 H, $-CH_2N(CO(CH_2)_2-CONHCH_2(CH_2)_3CH)CH_2-$), δ = 3.43 (dd, 4 H, $-N(CH_2COOC-(CH_3)_3)_2$), δ = 3.47 (m, 3 H, NBD-$N(CH_3)-$), δ = 4.04 (m, 2 H, NBD-$N(CH_3)CH_2-$), δ = 6.06 (d, 1 H, H-6), δ = 6.43 (b, 1 H, $-CO(CH_2)_2CONH-$), δ = 8.40 (d, 1 H, H-5). ^{13}C NMR (100 MHz, $CDCl_3$): δ = 14.74 (CH_3-), δ = 23.31, 23.84, 27.31−30.77, 32.35, 32.55, 39.98 ($H_3C(CH_2)_{16}CH_2N(CO(CH_2)_2CONHCH_2(CH_2)_3)CH_2-(CH_2)_{10}-$, $((CH_3)_3COCO-)_3$), δ = 42.15 (NBD-$N(CH_3)-$), δ = 46.86 ($CO(CH_2)_2CONHCH_2-$), δ = 48.61 ($-CH_2N(CO(CH_2)_2CONHCH_2-(CH_2)_3)CH_2-$), δ = 54.49 ($-N(CH_2COOC(CH_3)_3)_2$), δ = 56.63 (NBD-$N(CH_3)CH_2-$), δ = 65.76 ($-CO(CH_2)_2CONH(CH_2)_3(CH_2)CH-$), δ = 81.31 ($-N(CH_2COOC(CH_3)_3)_2$), δ = 81.69 ($(CH_3)_3COCOCH-$), δ = 101.55 (C-6), δ = 122.74 (C-5), δ = 136.00 (C-1), δ = 145.16 (C-2), δ = 145.52 (C-3), δ = 146.09 (C-4), δ = 171.34 ($-N(CH_2COOC-(CH_3)_3)_2$), δ =171.99 ($-CO(CH_2)_2CONH-$), δ = 173.00 ($(H_3C)_3-COCOCH-$), δ = 173.24 ($-CO(CH_2)_2CONH-$). MS (FAB, $C_{63}H_{112}-N_7O_{11}$): M + H^+ = 1143 *m/z*.

Synthesis of N^{α},N^{α}-Bis(carboxymethyl)-N^{ϵ}-(*N*-(*N*′-methyl-*N*′-(7-nitro-2,1,3-benzoxadiazol-4-yl)-12-aminododecyl)octadecylamine)-succinyl-L-lysine (13). Under the exclusion of light, 1005 mg (0.88 mmol) of compound **12** was dissolved in 90 mL of chloroform/trifluoroacetic acid (5:1). The reaction was stirred for 20 h at room temperature and then extracted twice with 1 N NaOH. After recrystallization from acetone, the product is purified by silica gel column chromatography with $CHCl_3$/MeOH/H_2O (69:27:4) as the eluant. Yield: 729 mg (0.75 mmol) of **13**, 81%. TLC: R_f = 0.38 in $CHCl_3$/MeOH/H_2O (69:27:4). ^{1}H NMR (400 MHz, $CDCl_3$/CD_3OD/F_3CCOOD (9:0.9:0.1): δ = 0.73 (t, 3 H, $H_3C(CH_2)_{17}-$), δ = 1.05−1.56 (m, 54 H, $H_3C(CH_2)_{16}-$, NBD-$N(CH_3)(CH_2)_2(CH_2)_9-$, $-CO(CH_2)_2CONHCH_2-(CH_2)_2-$), δ = 1.58−1.76 (m, 4 H, NBD-$N(CH_3)(CH_2)CH_2-$, $-CO(CH_2)_2CONH(CH_2)_3CH_2-$), δ = 2.34, 2.50 (2 t, 2*2 H, $-CO(CH_2)_2CONH-$), δ = 3.04 (m, 2 H, $-CO(CH_2)_2CONHCH_2-$), δ = 3.12 (m, 4 H, $-CH_2N(CO(CH_2)_2CO)CH_2-$), δ = 3.30 (t, 1 H, $-CO(CH_2)_2CONH(CH_2)_4CH-$), δ = 3.36 (m, 3 H, NBD-$N(CH_3)-$), δ = 3.45 (m, 4 H, $-^+NH(CH_2CO_2H)_2$), δ = 3.94 (m, 2 H, NBD-$N(CH_3)CH_2-$), δ = 6.03 (d, 1 H, H-6), δ = 8.32 (d, 1 H, H-5), ^{13}C NMR (100 MHz, $CDCl_3$/CD_3OD/F_3CCOOD (9:0.9:0.1): δ = 14.34 (H_3C-), δ = 23.06, 24.14, 27.04−30.07, 31.60, 32.32, 39.29, 46.97, 48.31−50.12 ($(H_3C(CH_2)_{17}N(CO(CH_2)_2CONH(CH_2)_4)(CH_2)_{11}-$, NBD-$N(CH_3)-$), δ = 55.55 ($-^+NH(CH_2CO_2H)_2$), δ = 56.51 (NBD-$N(CH_3)CH_2-$), δ = 66.48 ($-CO(CH_2)_2CONH(CH_2)_4CH-$), δ = 101.79 (C-6), δ = 121.95 (C-5), δ = 136.36 (C-1), δ = 145.12 (C-2), δ = 145.37 (C-3), δ = 146.32 (C-4), δ =172.70 ($-CO(CH_2)_2-$CONH−), δ =173.88 ($-CO(CH_2)_2CONH-$), δ = 175.49 ($-^+NH-(CH_2CO_2H)_2$), δ = 175.91 (HO_2CCH).

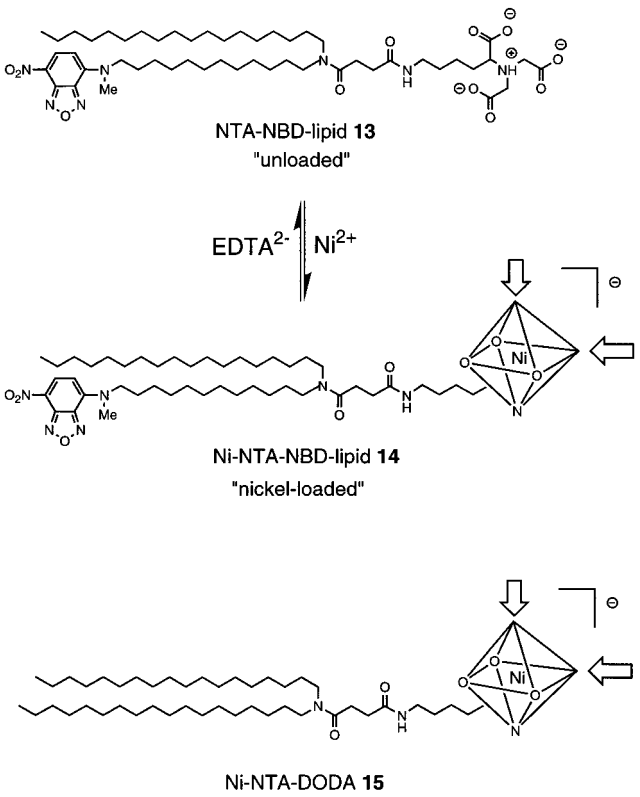

Figure 1. Chemical structure of the NBD-labeled chelator lipid **13** forming an octahedral complex (schematic) in the presence of nickel **14**. Arrows indicate the free binding sites which can be occupied by histidines. For comparison, the structure of the unlabeled chelator lipid **15** is illustrated.

Results and Discussion

Synthesis of Fluorescence-Labeled Chelator Lipids. A variety of biochemical and biophysical methods are known to study adsorption processes at lipid interfaces. However, in many cases, it is not possible to distinguish between adsorption of molecules to an interface on one hand and molecular recognition of a molecule by a particular lipid in the assembly on the other hand. Fluorescence energy transfer is well suited to monitor pair formation due to the distance dependency of energy transfer in the lower nanometer range. Thus, binding of an acceptor-labeled biomolecule to a donor-labeled lipid can be followed directly.

For our studies, we synthesized a metal-chelating lipid carrying a fluorophore as a spectroscopic reporter (Figure 1). To avoid interactions between the fluorophore and the metal-chelating group we used NBD, which is supposed to stay in the hydrophobic moiety of a lipid layer, whereas the NTA group is accessible to water. We decided in favor of a NBD label because of its spectral overlap and comparable fluorescence lifetime to the acceptor fluorophore rhodamine which was used to label the histidine-tagged molecule. In addition to its spectral properties, NBD is highly suitable for fluorescence recovery after photobleaching (FRAP) experiments to determine lateral diffusion in lipid interfaces.

The synthesis of lipid **13** is based on a modular system whereby the lipid backbone **1**−**8** is synthesized separately from the chelating headgroup **9**−**11** (Figure 2). Since the NBD fluorophore had to be introduced in the hydrophobic moiety of the lipid, we synthesized the asymmetrically substituted second-

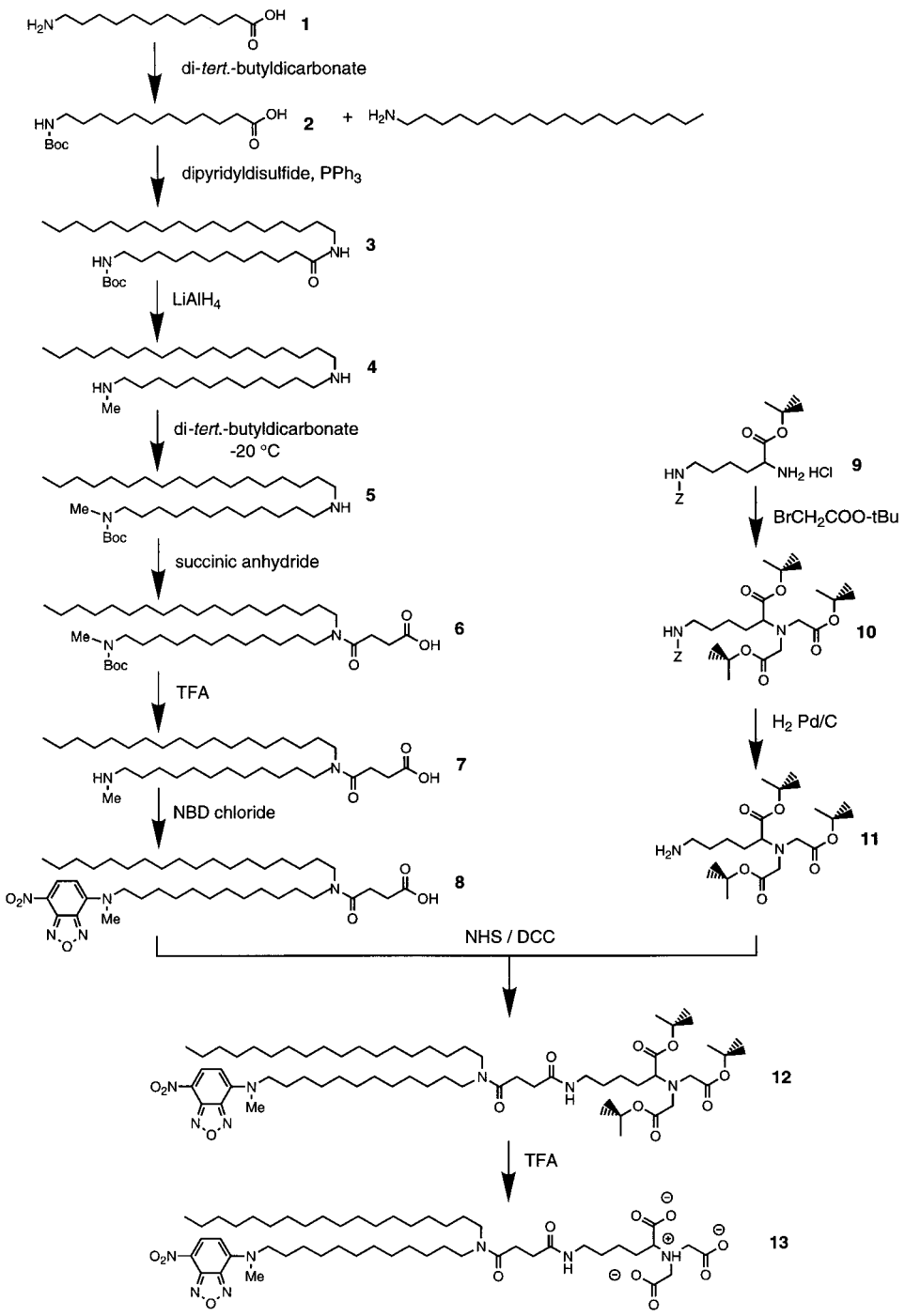

Figure 2. Synthesis of the NBD-labeled metal-chelating lipid **13**.

ary amine **5**. This was accomplished via reduction of the corresponding amide **3**. Problems occurred during reduction of the amide beside the carbamate of the Boc group in compound **3**. In contrast to amides substituted with shorter alkyl chains,[40] the reduction of the amide in compound **3** either failed or resulted in complex mixtures of products using selective reduction agents such as $(Bu)_4NBH_4$,[41] $NaBH_3OCOCF_3$,[42] $LiBH_4$/TMSCl,[43] $LiAlH_{4-n}(OMe)_n$,[44] or BH_3/THF.[45] We finally succeeded in quantitative reduction of the amide with the strong reducing agent $LiAlH_4$, but with the side effect of loosing the Boc protecting group at the primary amine. Interestingly, the release of the Boc group did not result in the primary amine as expected. Instead, quantitative methylation of the primary amine was observed. Although reductive alkylation of amines such as the Leuckart−Wallach reaction are extensively described,[40] methylation of primary amines via reduction of a Boc group was not reported so far. The reduction of the Boc group was verified by IR spectroscopy where no carbonyl valence vibration either of an amide or a carbamate were detected (data not shown). Reductive methylation of the primary amine was

(40) Glaser, H.; Möller, F.; Pieper, G.; Schröter, R.; Spielberger, G.; Söll, H. *Methoden der organischen Chemie (Houben-Weyl)*; Georg Thieme Verlag: Stuttgart, Germany, 1957; Vol. XI.

(41) Wakamatsu, T.; Inaki, H.; Ogawa, A.; Watanabe, M.; Ban *Heterocycles* **1980**, *14*, 1437−1440.

(42) Umino, N.; Iwakuma, T.; Itho, N. *Tetrahedron Lett.* **1976**, *33*, 2875−2876.

(43) Giannis, A.; Sandhoff, K. *Angew. Chem.* **1989**, *101*, 220−222.

(44) Brown, H. C.; Tsukamoto, A. *J. Am. Chem. Soc.* **1964**, *86*, 1089−1095.

(45) Roeske, R. W.; Weitl, F. L.; Prasad, K. U.; Thompson, R. M. *J. Org. Chem.* **1976**, *41*, 1260−1261.

demonstrated: (i) by mass spectrometry, where the masses of compounds **4**−**8** and **12** were increased by 14 amu ($RNHCH_3$ instead of RNH_2); (ii) by the high-resolution ^1H NMR spectra of **4**−**8**, **12**, and **13**, where a singlet with an integration of three protons was observed with a chemical shift depending on the substitution of the amine (**4**: $\delta = 2.43$ ppm, no substituent; **5**: $\delta = 2.83$ ppm, Boc group; **7**: $\delta = 2.64$ ppm, protonated; **8** and **12**: $\delta = 3.48$ and 3.47 ppm, NBD); (iii) by thin-layer chromatography, where the diamine **4** could not be stained with fluorescamine, a specific reagent for primary amines.[46] If the primary amine group in amide **3** was deprotected prior to reduction with $LiAlH_4$, neither a shift in the masses of **4**−**8**, **12**, and **13** by 14 amu nor a singlet with an integration of three protons in the ^1H NMR spectra was observed (data not shown). In this case the reduction product could be stained with fluorescamine.

In the next step, we had to reintroduce regioselectively the Boc group at the methyl-substituted amine in compound **4**. This was accomplished at −20 °C, whereas at higher temperatures or with an excess of di-*tert*-butyl dicarbonate, both amines were protected (data not shown). The following steps, coupling of the succinyl spacer and the NBD group, are described in the literature.[47,48]

The NTA derivative **11** was synthesized according to ref 23 but with a slight modification. The carboxy groups of NTA were protected by *tert*-butyl esters which leads to a better solubility of compound **11** in organic solutions and consequently to better yields in the coupling of the lipid backbone **8** with the chelator headgroup **11** (90%). In the final step, the *tert*-butyl esters are cleaved with TFA and the product is isolated by silica gel chromatography with an overall yield of 38%.

Pair Formation at the Monolayer Interface. The physical behavior of lipid monolayers at the air−water interface can be studied sensitively by film balance techniques. Molecular packing of the lipids as well as docking of biomolecules onto monolayers can be followed by changes in the area−pressure isotherms in parallel to a variety of surface-sensitive techniques. However, by using these methods, it is not possible to distinguish between adsorption to a monolayer and formation of a distinct lipid−protein complex. To follow the recognition process between histidine-tagged biomolecules and metal-chelating lipids, we studied the pair formation of a rhodamine-labeled histidine peptide and the synthesized NBD-labeled chelator lipid at the air−water interface by fluorescence resonance energy transfer. For these studies we designed a peptide composed of a C-terminal affinity tag of six histidines, a hydrophilic and flexible glycine-serine spacer, and a N-terminally coupled rhodamine fluorophore circumventing steric, hydrophobic, or electrostatic contribution caused, e.g., by a protein.

For the monolayer experiments, we chose SOPC as a matrix lipid because of its high fluidity over a broad range of lateral pressure and its length of alkyl chains matching best the alkyl chains of the labeled chelator lipid. The SOPC monolayer was doped with 3 mol % NBD-labeled Ni−NTA lipid **14**, and an area−pressure isotherm was recorded whereby a continuous transition from the liquid-expanded to the liquid-condensed phase was observed (data not shown). Up to 25 mN/m the monolayer shows a homogeneous fluorescence. Because of high lateral diffusion the fluorescence is recovered immediately after photobleaching of the fluorophore so that the NBD emission remains constant during the recording of the emission spectra (Figure 3a, solid line). At constant surface area, 1 nmol of rhodamine-labeled histidine peptide was added, yielding a final concentration of 40 nM in the subphase. Due to the high lateral pressure and the low molar ratio of metal-chelating lipid, only a slight increase in the lateral pressure of 0.5 mN/m was observed over a period of 2 h, which is in the range of error. In contrast to these minor thermodynamic changes of the lipid monolayer, a drastic effect on the fluorescence emission spectra was recorded after the addition of rhodamine-labeled histidine peptide. The NBD emission intensity at 530 nm decreased about 50%, and a new fluorescence band at 570 nm according to the emission maximum of rhodamine appeared (Figure 3a, dashed line). This decrease in donor intensity to the expense of the acceptor intensity provides strong evidence for a fluorescence energy transfer caused by direct binding of the rhodamine-labeled histidine peptide to the NBD-labeled chelator lipid. To provide further proof for a molecular recognition event, we added EDTA as a competitor for the nickel ion to the subphase. After the addition of EDTA to a final concentration of 0.1 mM,

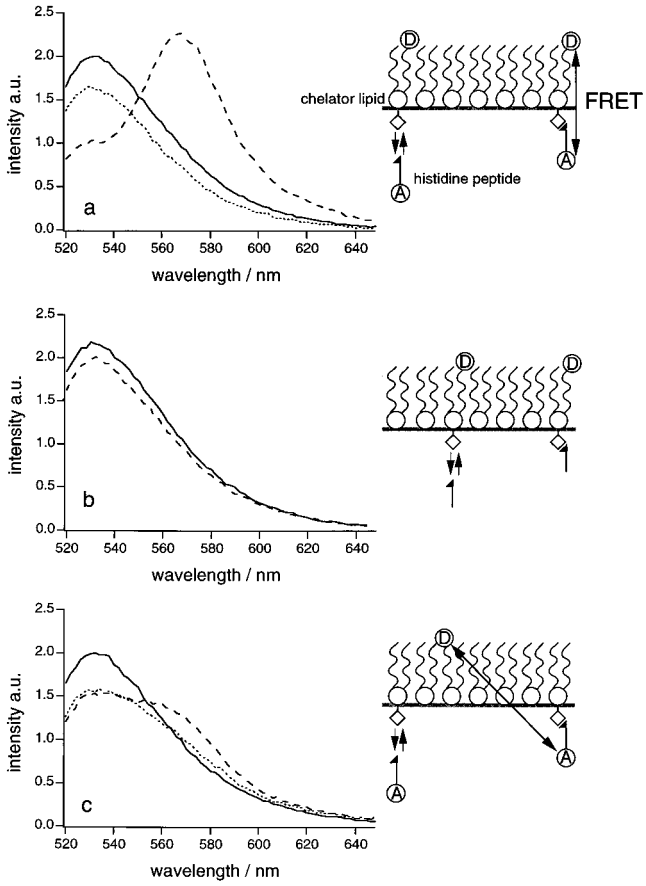

Figure 3. Fluorescence energy transfer at the air−water interface. Fluorescence emission spectra of a monolayer of (a) SOPC and 3 mol % of NBD-labeled Ni−NTA lipid **14** (solid line), after addition of 1 nmol (subphase concentration of 40 nM) of rhodamine-labeled histidine peptide (dashed line) and after addition of 100 μM EDTA to the subphase (dotted line), (b) SOPC and 3 mol % of NBD-labeled Ni−NTA lipid **14** (solid line) and after addition of 1 nmol of unlabeled histidine peptide (dashed line), (c) SOPC and 3 mol % of unlabeled Ni−NTA lipid **15** and 3 mol % of NBD-labeled lipid **8** (solid line), after the addition of 1 nmol of rhodamine-labeled histidine peptide (dashed line) and after the addition of 100 μM EDTA to the subphase (dotted line). All spectra were recorded at a lateral pressure of 20 ± 0.5 mN/m and on 10 mM HEPES, 150 mM NaCl, pH 7.5, at 22 °C.

(46) Udenfried, S.; Stein, S.; Böhlen, P.; Dairman, W. *Science* **1972**, *178*, 871−872.
(47) Kung, V. T.; Reedemann, C. T. *Biochim. Biophys. Acta* **1986**, *862*, 435−439.
(48) Gosh, P. B.; Whitehouse, M. W. *Biochemistry* **1968**, *108*, 155−159.

no rhodamine fluorescence was detected at the lipid interface and 80% of the NBD emission was recovered with respect to the beginning of the experiment (Figure 3a, dotted line). The loss of fluorescence intensity can be explained by bleaching of NBD at the air−water interface over a period of 6 h. In a comparable set of experiments, 1 nmol of unlabeled histidine peptide was injected underneath a monolayer of SOPC and 3 mol % NBD-labeled Ni−NTA lipid. Here again, the lateral pressure increased about 0.5 mN/m over a period of 2 h. In contrast to the experiment described before, the fluorescence emission decreased only by 10% (Figure 3b, dashed line) which is mainly due to NBD bleaching over the period of 2 h.

As final proof for pair formation between the histidine peptide and the metal-chelating lipid, 1 nmol of rhodamine-labeled peptide was injected underneath a monolayer identical to the experiments described before but with one exception. In this case, the fluorescence donor and the chelating group were not located within the same lipid. Here, the SOPC monolayer was doped with 3 mol % of unlabeled chelator lipid **15** and 3 mol % of NBD lipid **8**. After addition of the rhodamine-labeled histidine peptide, the lateral pressure again increased about 0.5 mN/m. The NBD emission decreased about 25%, and a small shoulder at 570 nm according to the rhodamine emission maximum was observed (Figure 3c, dashed line). Addition of EDTA to the subphase (0.1 mM) reduced the intensity at 570 nm (Figure 3c, dotted line) and increased the intensity at 530 nm only about 5%, indicating a much lower energy transfer efficiency in comparison to the first set of experiments with the fluorescent chelator lipid (for comparison see Figure 3a). This can be explained by a larger average distance of donor and acceptor since the chelator group and the fluorescence label are not linked to the same lipid. Thus, direct docking of the histidine peptide to the chelator lipid can be clearly distinguished from adsorption of the histidine peptide to a chelator lipid interface by the fluorescence energy transfer efficiency.

In all experiments the reversibility of the peptide binding could be demonstrated by adding EDTA to the subphase as competitor for the nickel. In both experiments energy transfer was reduced after injection of EDTA (Figure 3a,c, dotted lines). Although the rhodamine fluorescence vanished in Figure 3a, rhodamine fluorescence at the monolayer can still be detected in Figure 3c, indicating that there is still rhodamine-labeled peptide immobilized at the monolayer. This may be due to the higher amount of negatively charged lipids, 3 mol % of NTA lipid and 3 mol % of NBD lipid **8**, in the monolayer interacting electrostatically with the histidine tag because at pH 7.5 a small percentage of histidines are still positively charged. The reversibility of the binding was also demonstrated by an increase in NBD intensity after addition of EDTA. But in both experiments only 80% of the NBD intensity was recovered with respect to the intensity before addition of the rhodamine-labeled peptide. This decrease of the NBD fluorescence in the monolayer is most probably due to bleaching processes rather than fluorescence energy transfer.

Molecular Docking at Vesicles. Vesicles as mimics for cells, organelles, or biomembranes are well suited to study molecular recognition processes at membranes. Furthermore, in vesicle solution, the direct binding process of the rhodamine-labeled peptide to the NBD-labeled chelator lipid can be quantitatively analyzed by fluorescence energy transfer because bleaching of the dyes was not observed and the absorbance of the fluorophore can be measured precisely. For comparison and because of its ideal mixing and phase behavior, SOPC was chosen as matrix lipid. SOPC vesicles are unilamellar (100 nm in diameter) and in a fluid phase at room temperature.[49]

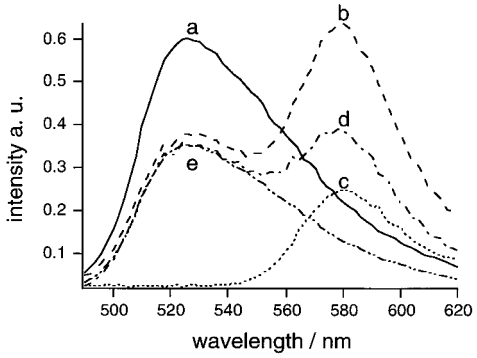

Figure 4. Fluorescence energy transfer in vesicle solution. Fluorescence emission spectra of SOPC vesicles containing: (a) 3 mol % of NBD-labeled Ni−NTA lipid **14**, (b) 3 mol % of NBD-labeled Ni−NTA lipid **14**, and 10 μM rhodamine-labeled histidine peptide, (c) 3 mol % of unlabeled Ni−NTA lipid **15** and 10 μM rhodamine-labeled histidine peptide. Spectrum c was subtracted from spectrum b to correct for direct rhodamine excitation resulting in spectrum d. Spectrum e is calculated by multiplying spectrum a by a factor of 0.54 to check for reabsorption from unbound rhodamine.

Molecular docking of the histidine peptide to the chelator lipid was demonstrated by a decrease in donor intensity and an increase in acceptor intensity induced by fluorescence energy transfer (Figure 4). To take the direct excitation of the rhodamine into account, a spectrum of rhodamine-labeled histidine peptide in the presence of unlabeled Ni−NTA lipid vesicles (Figure 4, spectrum c) was recorded and subtracted from the spectrum of NBD-labeled Ni−NTA lipid vesicles in the presence of rhodamine-labeled histidine peptide (Figure 4, spectrum b). The resulting difference spectrum (Figure 4, spectrum d) confirms an efficient fluorescence energy transfer from the donor-labeled chelator lipid to the acceptor-labeled histidine peptide. A decrease of NBD intensity induced by reabsorption from unbound rhodamine peptide can be excluded due to the unchanged shape of the NBD emission spectrum up to 540 nm. This is demonstrated by the comparison of spectrum d with spectrum e, which was calculated from a spectrum of NBD-labeled chelator lipid in the absence of rhodamine-labeled peptide (Figure 4, spectrum a) by adjusting same intensities at the NBD maximum.

We also checked the possibility that the binding of the histidine peptide could induce phase separation or structural reorganization of the fluorescence-labeled chelator lipid and thereby change the spectral properties of the fluorophore. First, we titrated SOPC vesicles containing 3 mol % of NBD-labeled Ni−NTA lipid with up to 10 μM of unlabeled histidine peptide. The intensity of the NBD remained unchanged within the range of error (data not shown), indicating that quenching of the donor emission by other effects besides fluorescence energy transfer can be excluded. Second, we checked for self-quenching by preparing SOPC vesicles which contain an increasing molar ratio of the fluorescent chelator lipid. We observed a linear dependency of the NBD fluorescence intensity up to 3 mol % (Figure 5), indicating that no self-quenching of the NBD occurs at molar ratios chosen in the experiments.

To determine a binding constant of histidine-tagged biomolecules for chelator lipids, we titrated SOPC vesicles containing 3 mol % of NBD-labeled chelator lipid with rhodamine-labeled histidine peptide. Energy transfer efficiencies were calculated

(49) Cevc, G. *Phospholipids Handbook*; Marcel Dekker Inc.: New York, 1993.

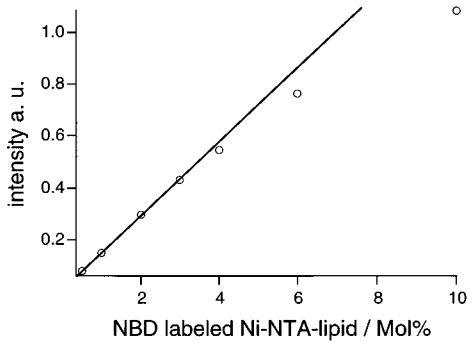

Figure 5. Fluorescence emission intensities at 530 nm of SOPC vesicles containing various amounts of NBD-labeled Ni−NTA lipid **14**. The linear regression curve is fitted to the first four values and then extrapolated.

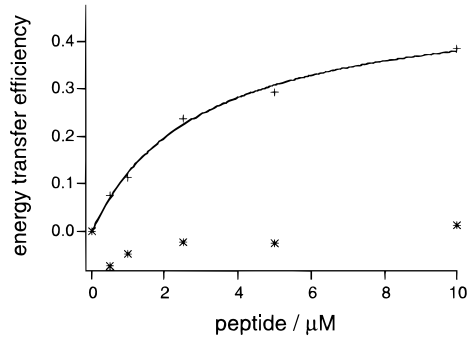

Figure 6. Binding constant of histidine peptide to vesicles doped with Ni−NTA lipid **14** was determined by fluoresecence energy transfer. Energy transfer efficiencies are plotted versus the concentration of rhodamine-labeled histidine peptide (i) for specific binding in the presence of Ni^{2+} (crosses) and (ii) for unspecific binding in the absence of Ni^{2+} (stars). The chelator lipid concentration was 3.25 μM, and measurements were performed in 10 mM HEPES, 150 mM NaCl, pH 7.5, at 22 °C. From the data a binding constant ($K_d = 3.0 \pm 0.4$ μM) was calculated.

from the decrease of donor intensities because an increase in acceptor intensity, especially at low acceptor concentrations, was difficult to observe. The fluorescence emission spectra were integrated from 490 to 540 nm to obtain a signal proportional to the relative quantum yield of the donor which is unaffected by the acceptor spectra. No change in the molar absorbance of the donor during the titration of the peptide occurred (data not shown). Therefore, we calculated the energy transfer efficiencies ET according to eq 4, where I and I_0 correspond to the

$$\mathrm{ET} = 1 - (I/I_0) \tag{4}$$

integrated fluorescence intensity of the donor in the presence and absence of acceptor, respectively. Assuming a two-state model of free and lipid-bound acceptor molecules, the energy transfer efficiency is proportional to the amount of acceptor-labeled histidine peptide bound to the donor-labeled NTA-lipid.[50] We plotted the energy transfer efficiencies against the concentration of rhodamine-labeled histidine peptide (Figure 6, crosses). The experimental data can be fitted by a Langmuir isotherm (Figure 6, solid line)

$$\mathrm{ET} = \frac{[\mathrm{A}]\mathrm{ET}_\infty}{K_d + [\mathrm{A}]} \tag{5}$$

where [A] corresponds to the total concentration of the peptide, K_d to the dissociation constant, and ET to the energy transfer efficiency at saturation. In the model, independent binding sites are assumed which seem to be reasonable at receptor concentration of 3 mol %. From the fit a dissociation constant K_d of 3.0 $\pm$ 0.4 μM was determined.

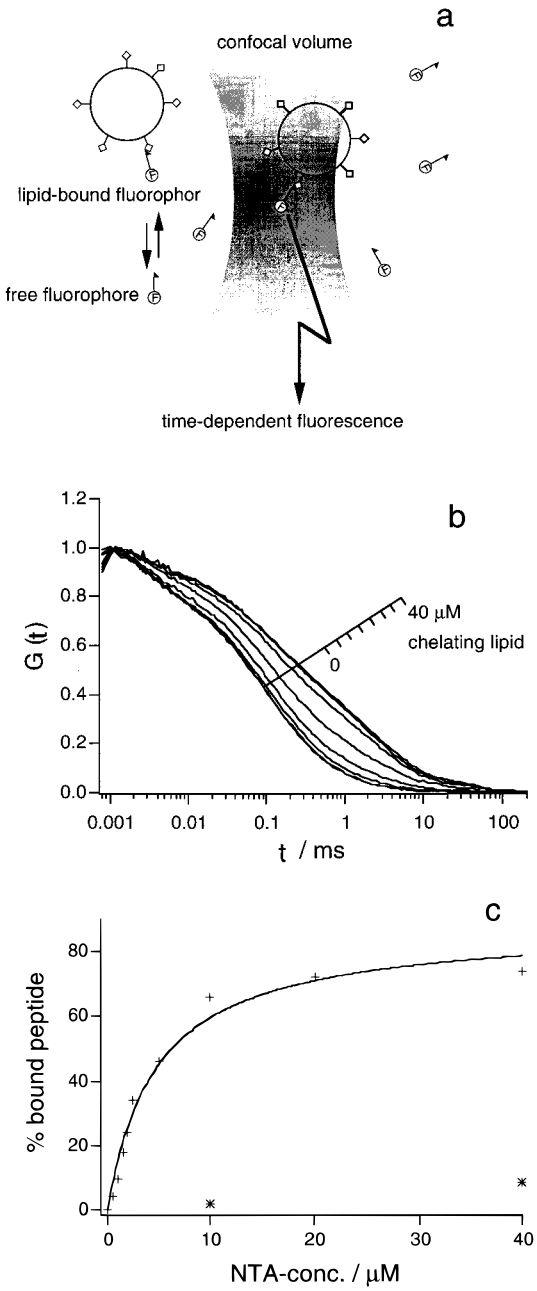

Figure 7. Fluorescence correlation spectroscopy. (a) Time-dependent fluorescence signal of rhodamine-labeled histidine peptides (15 nM) was analyzed regarding to their different diffusion times (τ) in the free or lipid-bound state. (b) Fluorescence autocorrelation functions $G(t)$ are shown in the presence of various amounts of SOPC vesicles containing 3 mol % of the Ni−NTA lipid **14**. The concentration of metal-chelating lipid in the outer vesicle leaflet is given (0, 0.5, 1, 2.5, 5, 10, 20, and 40 μM). The autocorrelation functions are normalized to an equal number of molecules in the confocal volume. (b) The fraction of bound peptide is calculated from the autocorrelation functions by a two-component fit and plotted versus the chelator lipid concentration which is accessible by the histidine peptide (outer vesicle leaflet). Experiments were performed in the presence (crosses) and absence of nickel ions (stars). The data are averaged from six measurements. From the data a binding constant ($K_d = 4.3 \pm 0.8$ μM) was calculated.

(50) Förster, T. *Z. Naturforsch.* **1949**, *4a*, 321−327.

Table 1. Diffusion Coefficients (D) Calculated from the Diffusion Time (τ) through the Confocal Volume (1.5 fL)[a]

fluorophore	τ (ms)	D (10^{-10}) (m^2 s^{-1})
rhodamine 6G (MW = 478)	0.07	2.8
histidine peptide (MW = 1976)	0.10	1.9
histidine peptide bound to vesicles (100 nm ∅)	2.4	0.08
latex bead (100 nm ∅)[39]		0.04

[a] Diffusion times t were calculated from a one- or two-component fit to the autocorrelation function of the time-dependent fluorescence signal.[39] The concentration of the fluorophore was 15 nM in 10 mM HEPES, 150 mM NaCl, pH 7.5, at 22 °C. The value of bound peptide was measured at saturation (40 μM Ni−NTA lipid **14**).

To check for unspecific binding of the rhodamine-labeled peptide, we performed the same experiment with SOPC vesicles containing unloaded chelator lipid in the presence of 0.1 mM EDTA. Even at peptide concentrations where saturation was reached in the specific binding experiment (10 μM), an energy transfer efficiency of only 3% was determined (Figure 6, stars).

In agreement with the monolayer experiments, an efficient fluorescence energy transfer was observed due to the binding of acceptor-labeled peptide to donor-labeled chelator lipid. The histidine peptide serves as an ideal model for the vast variety of histidine-tagged proteins since additional factors contributing to the specific binding process are kept minimal. Therefore, the binding constant (K_d = 3 μM) represents a standard value for the Ni−NTA system at self-assembled interfaces which can be increased or decreased by additional steric, electrostatic, or van der Waals contributions.

Fluorescence Correlation Spectroscopy. Alternatively, the binding constant of histidine-tagged molecules to metal-chelating lipids was examined by fluorescence correlation spectroscopy (FCS).[51] In contrast to the fluorescence energy transfer studies where the lipid acted as a spectroscopic reporter of the binding process, the rhodamine-labeled histidine peptide was used as a reporter in the FCS measurements. Therefore, the binding of the fast diffusing peptide to the slow diffusing SOPC vesicles containing 3 mol % Ni−NTA lipid was followed by FCS. To compare the results obtained from both methods, we used the unlabeled chelator lipid **15**, which has a structure very similar to that of the NBD-labeled chelator lipid (Figure 1). For the evaluation of the dissociation constant, we titrated 15 nM rhodamine-labeled histidine peptide with vesicles containing Ni−NTA lipid. From the fluorescence autocorrelation functions, which were normalized to an equal number of molecules in the confocal volume, an increase in the number of slow diffusing particles (bound peptides) was detected to the expense of the fast diffusing free peptides as the concentration of chelator lipid was increased (Figure 7a). The diffusion times τ and the diffusion coefficients D of free and lipid-bound molecules are given in Table 1. The diffusion constant of the rhodamine-labeled histidine peptide is slightly higher than for the standard rhodamine 6G according to the higher molecular weight or more precisely the larger hydrodynamic radius. Interestingly, the diffusion constant of the peptide bound to the vesicle (100 nm in diameter) is greater by a factor of 2 than the diffusion constant of a latex bead with the same diameter. The apparent faster diffusion of the vesicle bound fluorophore might be due to the additional lateral diffusion of the fluorophore in plane of the fluid membrane which does not occur with a fixed fluorophore on a latex bead. Moreover, vesicles and latex beads might differ in their hydrodynamic radii.

(51) Eigen, M.; Riegler, R. *Proc. Natl. Acad. Sci. U.S.A.* **1994**, *91*, 5740−5747.

The fraction of lipid-bound peptide was calculated from a two-component fit to the autocorrelation function of the time-dependent fluorescence signal (eq 2). This fraction was corrected for differences in the fluorescence quantum yield of bound and free peptide using eq 6, where c corresponds to the

$$c = \frac{y}{y + \alpha^2 - y\alpha^2} \tag{6}$$

corrected fraction of lipid-bound peptide, y to the measured fraction of lipid-bound peptide, and α to the ratio of counts per molecules (cpm) in the bound and free state (in this experiment α = 0.58).[39] The fraction of lipid-bound peptide was plotted against the chelator lipid concentration (Figure 7b). Similar to the fluorescence energy transfer measurements, the data can be fitted by a Langmuir isotherm

$$R = \frac{[A]R_\infty}{K_d + [A]} \tag{7}$$

where R is the fraction of lipid-bound peptide, R_∞ the fraction of bound peptide at saturation, K_d the dissociation constant, and [A] the concentration of NTA-lipid in the outer leaflet of the vesicle assuming an equal distribution of NTA lipid between the inner and outer leaflet. From the fit a dissociation constant K_d of 4.3 ± 0.8 μM was obtained. To check for unspecific binding, an identical experiment was performed with vesicles containing unloaded chelator lipid in the presence of 100 μM EDTA. Even at chelator lipid concentrations (40 μM) where saturation of the specific binding was observed, only 3.7% of the rhodamine-labeled peptide was bound to the vesicles.

The rather large difference in the diffusion coefficients of the free and the vesicle-bound ligand makes fluorescence correlation spectroscopy a well-suited method to study binding of ligands to lipid vesicles in a homogeneous assay. Although pair formation between histidine peptide and chelator lipid cannot be distinguished from peptide adsorption to chelator lipid containing vesicles, the very low unspecific binding of 3.7 % strongly suggests that direct binding of the histidine peptide to the chelator lipid assembled in SOPC vesicles occurs. The determined dissociation constant K_d of 4.3 ± 0.8 μM is in good agreement with the dissociation constant K_d of 3.0 ± 0.4 μM determined by fluorescence energy transfer.

Conclusion

The concept of metal-chelating lipids is a versatile and powerful method for the immobilization, orientation, and two-dimensional crystallization of proteins at self-organizing interfaces. In this study, molecular recognition of a rhodamine-labeled histidine peptide by a novel NBD-labeled chelator lipid was demonstrated using fluorescence energy transfer at the monolayer interface as well as in vesicle solution. Thereby we were able to distinguish between a direct binding of the histidine-tagged molecule to the chelator lipid and adsorption onto the lipid interface due to the distance dependency of energy transfer efficiency. The immobilization is highly specific, leading to only 3% unspecific binding. An affinity constant of 3 μM was determined by fluorescence energy transfer and by fluorescence correlation spectroscopy. In literature, binding of histidine-tagged proteins to immobilized NTA− or IDA−metal complexes is often characterized by a drastically higher affinity than measured in this report. These high affinity constants were not experimentally determined and mistaken for the formation of the metal−chelate complex. The simple and effective one-

step purification of histidine-tagged proteins by immobilized metal ion affinity chromatography (IMAC) is possibly due to the number of theoretical plates during chromatography allowing efficient rebinding after dissociation or from multivalent interactions of the tagged protein with the affinity matrix. In this report, the binding of histidine-tagged molecules to metal-chelating lipids diluted into a self-assembled lipid matrix was investigated. The affinity constant determined for the histidine peptide by two independent methods is in agreement to the binding constant of various histidine-tagged proteins analyzed (I.T.D. and R.T., unpublished results). Furthermore, these values are in the same range as the dissociation constant K_d of 1.5 μM reported for the binding of a histidine-tagged T-cell receptor to Ni−NTA thiols self-assembled on gold.[38] In another publication, saturation for the immobilization of a histidine-tagged polymerase to a Ni−NTA dextran surface was observed at 2 μM.[16] Despite the rather moderate dissociation constant, kinetically stable immobilization of the proteins at the chelator interfaces is reported for at least 60 min, demonstrating the suitability of the chelator concept for bioanalytical studies.[16,27,38] Detailed kinetic studies of the complex formation are under investigation.

Acknowledgment. We thank Drs. Lutz Schmitt, Ulf Raedler, Rudi Merkel, Joachim Rädler, and Erich Sackmann for helpful discussions and Drs. Wolfram Schäfer and Isolde Sonnenbichler for providing the MS and NMR spectra. We are grateful to Dr. B. Hecks (EVOTEC) and P. Bremer (Carl Zeiss Jena) for their support and helpful comments concerning the FCS measurements. This work was supported by the Deutsche Forschungsgemeinschaft and the Bundesministerium für Bildung und Forschung.

JA9735620